

# Clustering of Galaxies in a Hierarchical Universe: II. Evolution to High Redshift

Guinevere Kauffmann, Jörg M. Colberg, Antonaldo Diaferio & Simon D.M.  
White

*Max-Planck Institut für Astrophysik, D-85740 Garching, Germany*

## Abstract

In hierarchical cosmologies the evolution of galaxy clustering depends both on cosmological quantities such as  $\Omega$ ,  $\Lambda$  and  $P(k)$ , which determine how collapsed structures – dark matter halos – form and evolve, and on the physical processes – cooling, star formation, radiative and hydrodynamic feedback – which drive the formation of galaxies within these merging halos. In this paper, we combine dissipationless cosmological N-body simulations and semi-analytic models of galaxy formation in order to study how these two aspects interact. We focus on the differences in clustering predicted for galaxies of differing luminosity, colour, morphology and star formation rate, and on what these differences can teach us about the galaxy formation process. We show that a “dip” in the amplitude of galaxy correlations between  $z = 0$  and  $z = 1$  can be an important diagnostic. Such a dip occurs in low-density CDM models, because structure forms early and dark matter halos of mass  $\sim 10^{12}M_{\odot}$ , containing galaxies with luminosities  $\sim L_*$ , are unbiased tracers of the dark matter over this redshift range; their clustering amplitude then evolves similarly to that of the dark matter. At higher redshifts bright galaxies become strongly biased and the clustering amplitude increases again. In high density models, structure forms late and bias evolves much more rapidly. As a result, the clustering amplitude of  $L_*$  galaxies remains constant from  $z = 0$  to  $z = 1$ . The strength of these effects is sensitive to sample selection. The dip becomes weaker for galaxies with lower star formation rates, redder colours, higher luminosities and earlier morphological types. We explain why this is the case and how it is related to the variation with redshift of the abundance and environment of the observed galaxies. We also show that the relative peculiar velocities of galaxies are biased low in our models, but that this effect is never very strong. Studies of clustering evolution as a function of galaxy properties should place strong constraints on models of galaxy formation and evolution.

Keywords: galaxies: formation; galaxies:halos; cosmology:large-scale structure; cosmology: dark matter

# 1 Introduction

Local galaxies are highly clustered. On large scales they are organized into a network of sheets and filaments which surround large underdense regions, usually referred to as voids. On smaller scales galaxies are found in gravitationally-bound groups and clusters. According to the standard theoretical paradigm, the structures observed today were formed by the gravitational amplification of small perturbations in an initially gaussian dark matter density field. Small scale overdensities were the first to collapse, and the resulting objects subsequently merged under the influence of gravity to form larger structures such as clusters and superclusters. Galaxies formed within dense *halos* of dark matter, where gas was able to reach high enough overdensities to cool, condense and form stars.

In this hierarchical formation picture, the clustering of the dark matter, as measured by the amplitude of the matter correlation function  $\xi_m(r)$ , increases monotonically with time. The precise evolution of  $\xi_m(r)$  with redshift has been studied extensively using both N-body simulations (e.g. Jenkins et al. 1998) and analytic methods (Hamilton et al 1991; Peacock & Dodds 1994; Jain, Mo & White 1995). If  $\xi_m(r, z)$  were observable, it would be straightforward to use its behaviour to determine  $\Omega$ ,  $\Lambda$  and the power spectrum of linear density fluctuations. What one measures in practice, however, is the clustering of galaxies, and the interpretation then requires an understanding of how these objects trace the underlying dark matter density field.

If galaxies form at the centre of dark matter halos, considerable insight may be gained by using N-body simulations to study the clustering of halos (Brainerd & Villumsen 1994; Mo & White 1996; Roukema et al 1997; Jing & Suto 1998; Wechsler et al 1998; Bagla 1998a,b; Ma 1998). Mo & White (1996) tested an approximate analytic theory against their numerical results, and this theory and its extensions can also be used to analyse the evolution of halo clustering with redshift (Matarrese et al 1997; Coles et al 1998). An important conclusion from all these studies is that the clustering of halos of galactic mass ( $\sim 10^{12}M_\odot$ ) evolves much more slowly than the clustering of the dark matter. This is because at high redshifts, such halos correspond to rare peaks in the initial density field, and are thus more strongly clustered than the dark matter (Kaiser 1984). Another important conclusion is that more massive halos are more strongly clustered than less massive halos. If the luminosity of a galaxy is correlated with the mass of its halo, more luminous galaxies ought to be more strongly clustered. A detailed comparison with observational data requires a model for the observable properties of the galaxies present within halos of given mass at each epoch.

Precise measurement of the clustering amplitude of galaxies at high redshift has just recently become feasible. Usually this is done by calculating the angular two-point correlation function  $w(\theta)$  as a function of apparent magnitude. In order to assess how clustering has evolved,  $w(\theta)$  must be deprojected using Limber's equation under the assumption of some specific model for the redshift distribution of the observed galaxies. In future large surveys of faint galaxies with photometric and/or spectroscopic redshifts will be available (see, for example, Connolly et al 1995). It will be possible to classify the galaxies in these surveys according to absolute magnitude, spectral type, star formation rate and colour, and to investigate how clustering evolution depends on these properties.

At present, most of the data indicate that the clustering amplitude of galaxies *decreases* from  $z = 0$  to  $z = 1$ . Different analyses, however, yield very different estimates for the strength of this decrease. Le Fèvre et al (1996) analyzed the clustering of 591 galaxies with  $I < 22.5$  in the five 10 arcminute fields of the CFRS survey. They find that clustering has evolved dramatically, quoting a comoving correlation length at redshift 0.5 of  $r_0 = 2 \text{ h}^{-1} \text{ Mpc}$  ( $q_0 = 0.5$ ). More recently, Carlberg et al (1998) presented a preliminary analysis of clustering in the CNOC2 field galaxy redshift survey. Their sample is spread over four patches of sky with a total area of 1.5 square degrees. They estimate that the comoving correlation length of galaxies with  $M_R < -20$  evolves as  $r_0(z) = (5.15 \pm 0.15)(1+z)^{-0.3 \pm 0.2} \text{ h}^{-1} \text{ Mpc}$ . This is much weaker than the evolution found for the CFRS galaxies. The results of Carlberg et al (1998) agree reasonably well with those of Postman et al (1998), based on 710 000 galaxies with  $I_{AB} < 24$  from an imaging survey of a contiguous 4 square degree region of the sky. The latter authors suggest that the small volumes sampled by the CFRS and other early surveys resulted in their derived correlation lengths being biased low.

The clustering of Lyman break galaxies at  $z \sim 3$  has now been measured with surprising precision (Steidel et al 1998a; Giavalisco et al 1998; Adelberger et al 1998). The comoving correlation length of these objects is comparable to that of  $L_*$  galaxies today, implying, as expected from models of halo clustering, that Lyman break galaxies are highly biased tracers of the dark matter distribution at these redshifts. In addition, Giavalisco et al (1998) find that the fainter Lyman break galaxies are less strongly clustered. This accords well with a simple model in which the star formation rates in these objects increase with the mass of their halos. More detailed theoretical modelling of the observed properties of Lyman break galaxies at  $z = 3$ , including analysis of their abundances, sizes, luminosities, colours, star formation rates and clustering properties, has been carried out by Mo & Fukugita (1996), Baugh et al (1998), Governato et al (1998), Somerville, Primack & Faber(1998) and Mo, Mao & White (1998)

In this paper, we combine cosmological N-body simulations and semi-analytic modelling of galaxy formation to study the evolution of galaxy clustering as a function of redshift. Our methods for incorporating galaxy formation in the simulations are discussed in detail in Kauffmann et al (1998, Paper I). Two variants of a cold dark matter (CDM) cosmology are analyzed here: a high-density model with  $\Omega = 1$ ,  $\Gamma = 0.2$  and  $H_0 = 50 \text{ km s}^{-1} \text{ Mpc}^{-1}$  ( $\tau\text{CDM}$ ), and a low-density flat model with  $\Omega = 0.3$ ,  $\Lambda = 0.7$  and  $H_0 = 70 \text{ km s}^{-1} \text{ Mpc}^{-1}$  ( $\Lambda\text{CDM}$ ). Paper I was concerned with the global properties of the galaxy distribution at  $z = 0$ , including B and K-band luminosity functions, the I-band Tully-Fisher relation, galaxy two-point correlation functions, colour distributions, star formation rate functions and peculiar velocity distributions. Here we focus on clustering evolution in the two models. We study the predicted differences in clustering evolution for galaxies of different magnitude, type and star formation rate, and we outline how future observational data will clarify the galaxy formation process.

## 2 What can be learned from the evolution of halo clustering?

Because galaxy formation is complex and involves many poorly-understood physical processes, for example, star formation and radiative and hydrodynamical feedback, it is worthwhile to ask whether the clustering of dark matter halos can be used to constrain cosmological parameters directly.

In figure 1 we plot the correlation length  $r_0$  as a function of redshift for halos of different mass in our two simulations. Here, as in the rest of the paper, all length scales are expressed in comoving units. Since the correlation functions in the models are not exact power laws, we define  $r_0$  as the radius where  $\xi(r) = 1$ . The smallest halos resolved in the simulations contain 10 particles and have virial masses  $\sim 2 \times 10^{11} M_\odot$ . For these objects,  $r_0$  initially decreases with redshift, reaches a minimum, and then increases again. The redshift of this minimum is different for the two cosmologies:  $z \sim 0.7$  for  $\tau$ CDM and  $z \sim 1.5$  for  $\Lambda$ CDM. Massive halos do not exhibit the same “dip” in correlation length; their  $r_0$  remains constant for a while, then increases at high redshift. Once again, the redshift at which the evolution becomes strong is lower for  $\tau$ CDM than for  $\Lambda$ CDM. This is simply because structure formation occurs *later* in the  $\tau$ CDM model.

With 10 metre telescopes, it is now possible to measure the rotation curves of disk galaxies at redshift  $\sim 1$  (Vogt et al 1996). It will be many years, however, before such samples are both large enough and complete enough for an analysis of the clustering evolution of galaxies as a function of their halo mass. In all likelihood, we will have to deal with flux-limited surveys of galaxies for some time to come.

Let us now make the simplifying assumption that each simulated dark matter halo contains one observable galaxy, and that the luminosity of the galaxy increases with the mass of its halo. The correlation function of a flux-limited sample of galaxies *of known abundance* at redshift  $z$  may then be calculated by evaluating  $\xi(r)$  for the mass-limited set of simulated halos which has the same abundance. This is illustrated in figure 2, where we plot the correlation length of halos versus their number density (in units of  $h^3 \text{ Mpc}^{-3}$ ) at a series of redshifts. As expected,  $r_0$  decreases as the number density increases, because the correlation signal becomes dominated by low-mass halos, which are more weakly clustered. Note that the differences between the  $\tau$ CDM and the  $\Lambda$ CDM models are small at all redshifts. Mo, Mao & White (1998) show a similar plot for halos at  $z = 3$  for four different CDM cosmologies and find that they all give similar results. There thus appears to be a “cosmic conspiracy” that makes it impossible to infer information about cosmological parameters from the clustering of halos of given abundance. On the other hand, the uniformity seen in figure 2 can be used as a *test* of the entire class of hierarchical models and of the hypothesis that there is a one-to-one correspondence between halo mass and galaxy luminosity. As discussed by Steidel et al (1998b) and by Mo, Mao & White (1998), this hypothesis works well for the Lyman break population at  $z \sim 3$ . At low redshifts, the assumption of a one-to-one correspondence between halos and galaxies must break down, because the abundance of high mass halos is larger, and more and more bright galaxies are grouped together in each such halo. The values of  $r_0$  plotted in figure 2 are then lower limits on the true values.

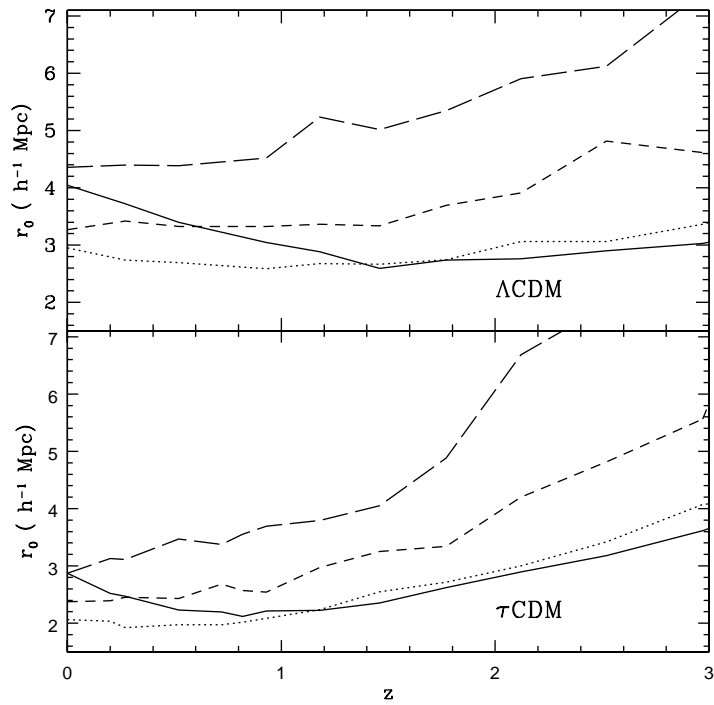


Figure 1: The evolution of the co-moving correlation length of halos as a function of redshift in the  $\tau$ CDM and  $\Lambda$ CDM simulations. The solid line is for halos with  $\log(M_{vir}/M_{\odot})$  in the range 11.0 – 11.5, the dotted line for 11.5 – 12, the short-dashed line for 12 – 12.5 and the long-dashed line for 12.5 – 13.

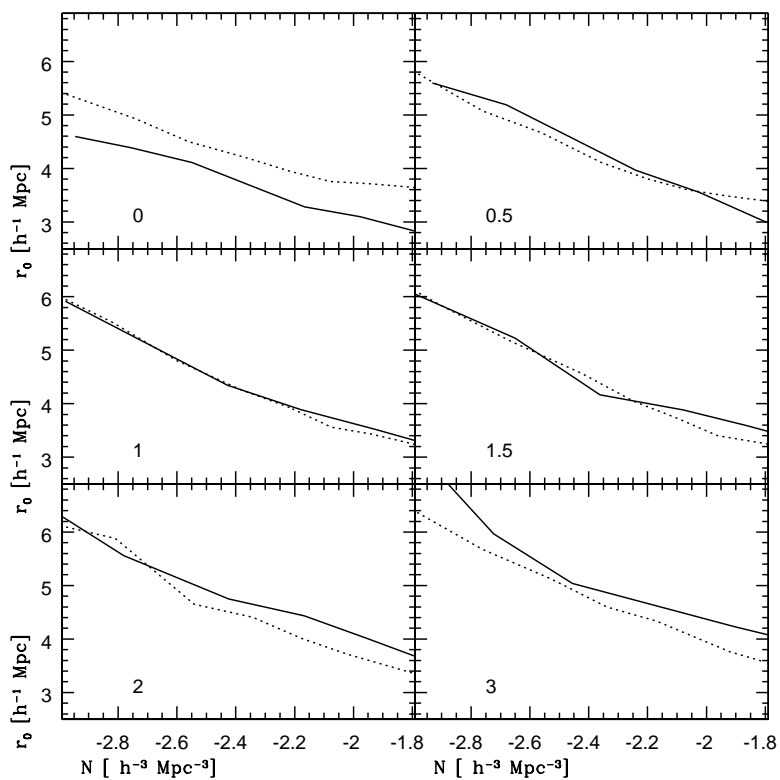


Figure 2: The co-moving correlation length  $r_0$  of halos is plotted against comoving number density at redshifts 0, 0.5, 1, 1.5, 2 and 3. The solid line shows results for the  $\tau\text{CDM}$  simulation and the dotted line for the  $\Lambda\text{CDM}$  simulation.

### 3 The evolution of galaxy clustering

In this section, we study the evolution of galaxy clustering in the  $\Lambda$ CDM and  $\tau$ CDM simulations. We use the star formation and feedback recipes that resulted in the best fits to the observational data at  $z = 0$ . As discussed in Paper I, extremely efficient feedback was required in the  $\tau$ CDM model in order to obtain a reasonable fit to the correlation function on scales below  $1 \text{ h}^{-1} \text{ Mpc}$  and to avoid producing too many galaxies with luminosities below  $L_*$ . Even so, the model failed to fit the observed bright end of the luminosity function and the clustering amplitude was too low on large scales. The  $\Lambda$ CDM model with relatively inefficient feedback resulted in a better overall fit to most of the data at  $z = 0$ . For simplicity, we do not consider dust extinction in the analysis of this paper because it is very uncertain how the empirical recipes we adopted in Paper I should be extended to high redshift. This neglect has little effect on our  $\Lambda$ CDM model but means that our  $\tau$ CDM model now substantially underpredicts galaxy clustering at  $z = 0$ . We concentrate below on the relative evolution of  $r_0$  rather than on its absolute value, so this problem does not strongly affect our conclusions.

In figure 3 results are shown for galaxies with rest-frame B-band magnitudes brighter than  $-19 + 5 \log h$  in the  $\Lambda$ CDM simulation. At redshift zero, this corresponds to selecting galaxies brighter than  $\sim L_*$ . The first three panels in the plot show the evolution of  $\xi(r)$  evaluated at  $r = 2, 3$  and  $8 \text{ h}^{-1} \text{ Mpc}$  (co-moving units). The fourth panel shows the evolution of the co-moving correlation length  $r_0$ . For comparison, the dotted line in each panel shows the evolution of the corresponding quantity for the dark matter. Results for  $\tau$ CDM are given in figure 4. In each case the redshift extends to the point at which the abundance of  $L_*$  galaxies becomes too low for reliable estimation of the correlation function.

In the  $\Lambda$ CDM model, the clustering amplitude decreases from  $z = 0$  to  $z = 1.5$ , remains approximately constant from  $z = 1.5$  to  $z = 2.5$  and then increases again at higher redshift. The dip in clustering amplitude is stronger on small scales:  $\xi(r)$  decreases by a factor of 3 at  $2 \text{ h}^{-1} \text{ Mpc}$  and by a factor 1.5 at  $8 \text{ h}^{-1} \text{ Mpc}$ . The correlation length  $r_0$  decreases from  $5.5 \text{ h}^{-1} \text{ Mpc}$  at  $z = 0$  to  $3.9 \text{ h}^{-1} \text{ Mpc}$  at  $z = 1.5$ . This agrees remarkably well with the parametrization of  $r_0$  as a function of  $z$  quoted by Carlberg et al (1998). In the  $\tau$ CDM model the clustering amplitude remains fixed from  $z = 0$  to  $z = 1$  and then rises steeply at higher redshifts. Note, as mentioned above, that the correlation length at  $z = 0$  is low ( $\sim 3 \text{ h}^{-1} \text{ Mpc}$ ) in this model.

In figure 5, we plot the evolution of the bias  $b$ , defined as the square root of the ratio between the galaxy and the dark matter correlation functions:

$$b(r) = \left( \frac{\xi_g(r)}{\xi_m(r)} \right)^{1/2}. \quad (1)$$

The four lines on the plot show the bias as a function of redshift evaluated at  $r = 2, 3, 5$  and  $8 \text{ h}^{-1} \text{ Mpc}$ . The bias does not depend on  $r$  in either model, except at very high redshifts where  $b$  is somewhat larger on small scales. The bias evolves much more rapidly in the  $\tau$ CDM model than in the  $\Lambda$ CDM model. Galaxies in the  $\Lambda$ CDM model are unbiased tracers of the mass out to  $z \sim 1$ . Galaxies in the  $\tau$ CDM model have bias values of about 2 at this redshift.

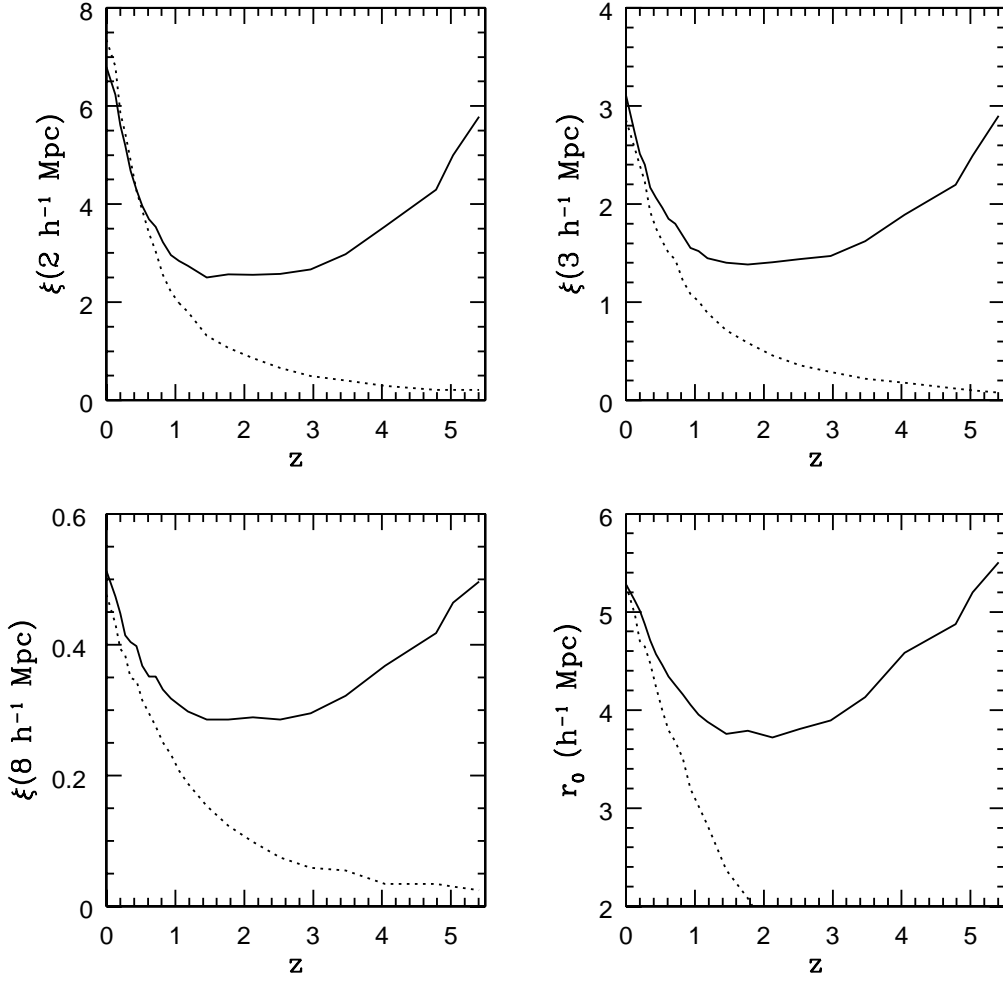


Figure 3: Evolution of clustering in the  $\Lambda$ CDM model. In the first 3 panels, the clustering amplitude is plotted against redshift for galaxies with rest-frame B-band magnitude brighter than  $-19 + 5 \log h$  (solid lines) and for the dark matter (dotted line). Results are shown for  $\xi(r)$  evaluated at  $r = 2, 3$  and  $8 \text{ h}^{-1} \text{ Mpc}^{-1}$ . In the fourth panel, the comoving correlation length  $r_0$  is plotted against redshift both for the galaxies and for the dark matter.

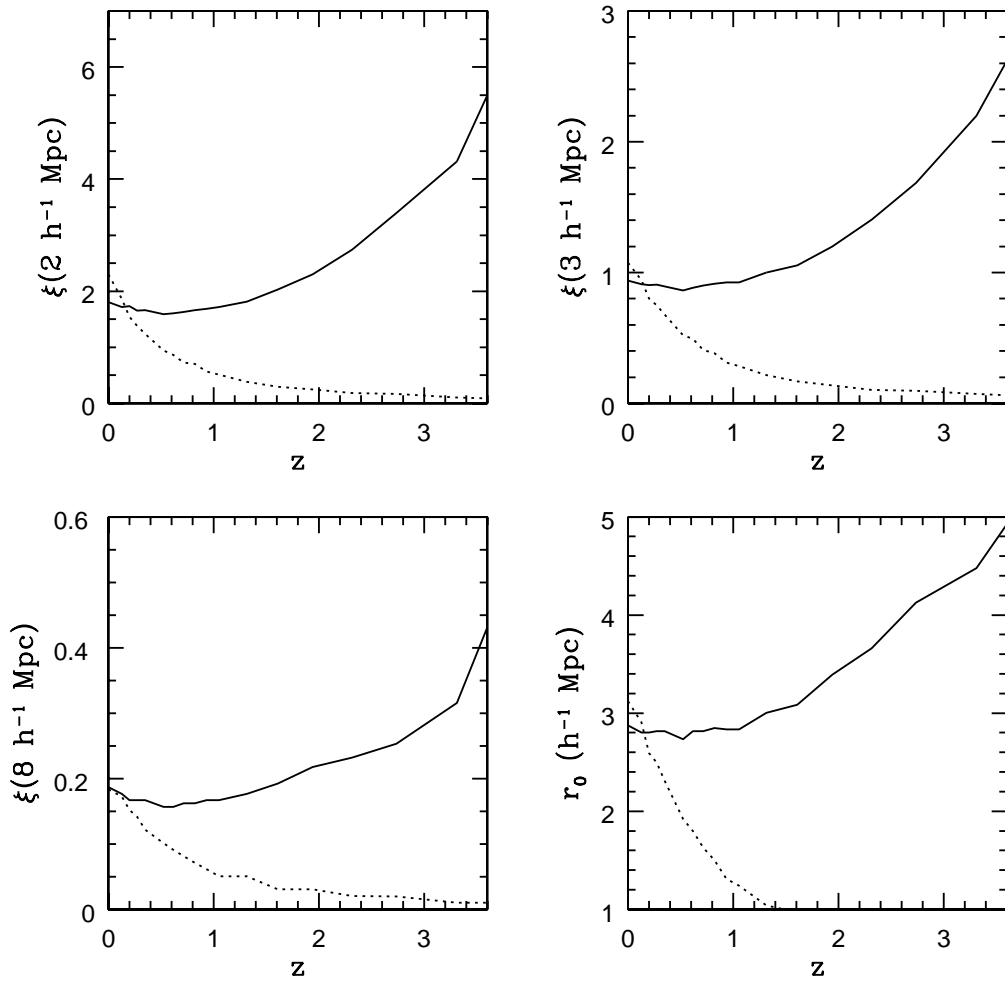


Figure 4: As in figure 3, except for the  $\tau$ CDM model.

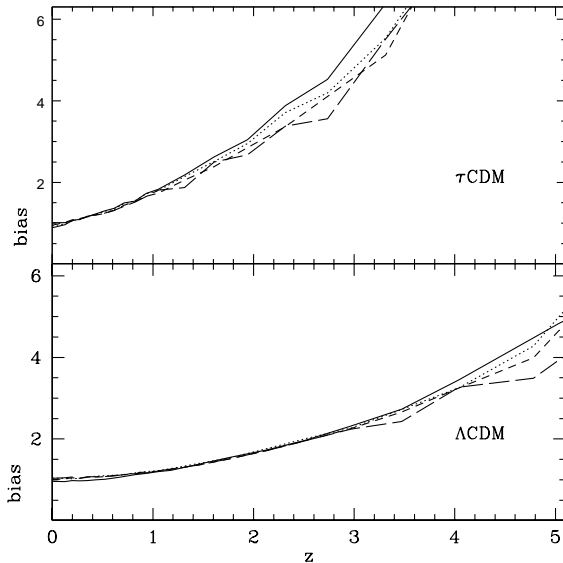


Figure 5: Evolution of the bias for galaxies with rest-frame B-band magnitude brighter than  $-19 + 5 \log h$  in the  $\Lambda$ CDM and  $\tau$ CDM models. Solid, dotted, short-dashed and long-dashed lines show results evaluated on comoving scales of 2, 3, 5 and  $8 h^{-1}$  Mpc respectively.

## 4 Dependence on luminosity, star formation rate and morphological type

In figures 6 and 7, we demonstrate that the clustering evolution depends on the way in which galaxies are selected in the simulations. The first panel compares the clustering evolution of galaxies selected in the rest-frame B-band with that of galaxies selected in the rest-frame I-band. The second panel compares the clustering evolution of galaxies with  $M(B) < -19 + 5 \log h$  with that of galaxies 1.5 magnitudes brighter. The third panel shows what happens if galaxies are selected by star formation rate rather than by luminosity. The fourth panel shows the clustering of early-type galaxies with stellar mass greater than  $3 \times 10^{10} M_{\odot}$  (recall from Paper I that these objects form by mergers of two galaxies of similar mass and have  $M(B)_{bulge} - M(B)_{total} < 1$  mag).

In the  $\Lambda$ CDM model, we find that the strength of the “dip” in clustering between  $z = 0$  and  $z = 1.5$  is sensitive to sample selection. The dip is weaker for more luminous galaxies and for galaxies selected in the I-band, but stronger for galaxies selected by star formation rate. The clustering amplitude of early-type galaxies is stronger than that of the population as a whole and evolves very little with redshift. In the  $\tau$ CDM model, clustering evolution is less sensitive to sample selection. The clustering always remains fixed out to  $z \sim 1$  and then rises steeply at higher redshifts. Early-type galaxies are also very strongly clustered in this model, particularly at high redshifts.

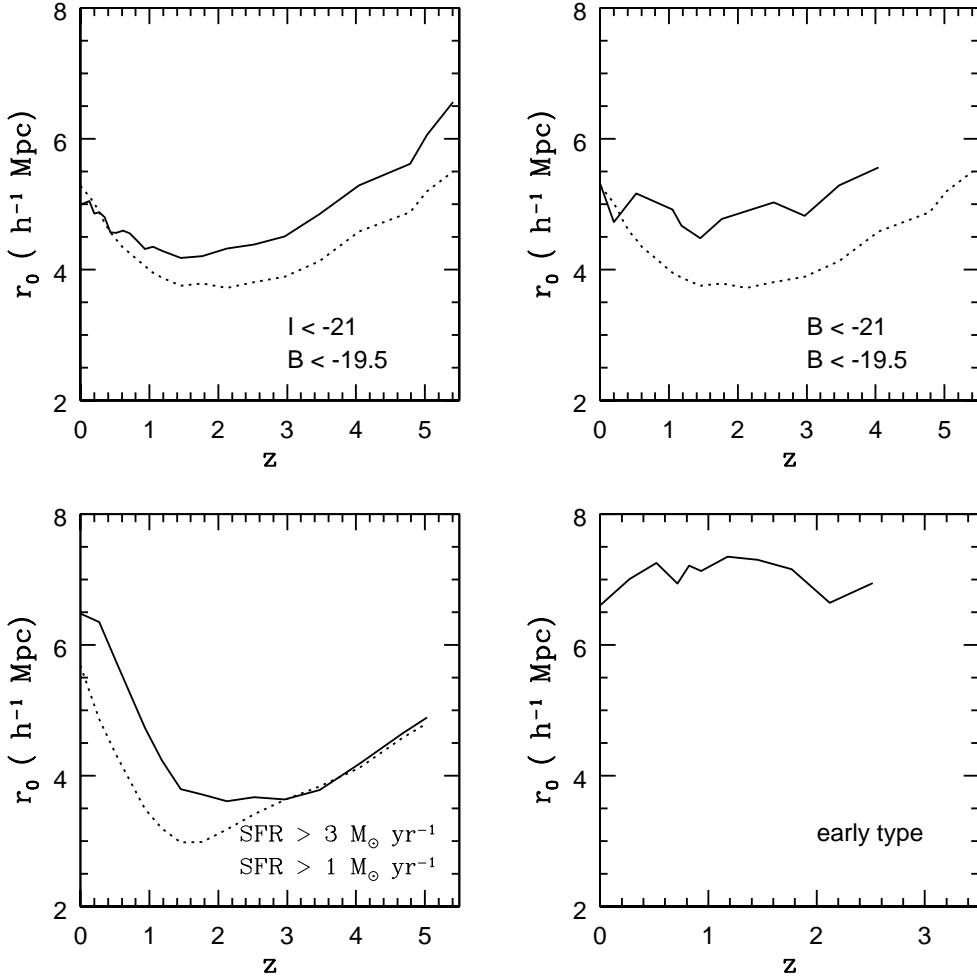


Figure 6: The dependence of clustering evolution on sample selection in the  $\Lambda$ CDM model. The comoving correlation length  $r_0$  is plotted as a function of redshift for: a)  $L_*$  galaxies selected in the rest-frame I-band (solid) and  $L_*$  galaxies selected in the rest-frame B-band (dotted); b) very bright galaxies (solid) and  $L_*$  galaxies (dotted); c) galaxies with star formation rate greater than  $3 M_\odot \text{ yr}^{-1}$  (solid) and  $1 M_\odot \text{ yr}^{-1}$  (dotted); d) early-type galaxies with stellar masses greater than  $3 \times 10^{10} M_\odot$ .

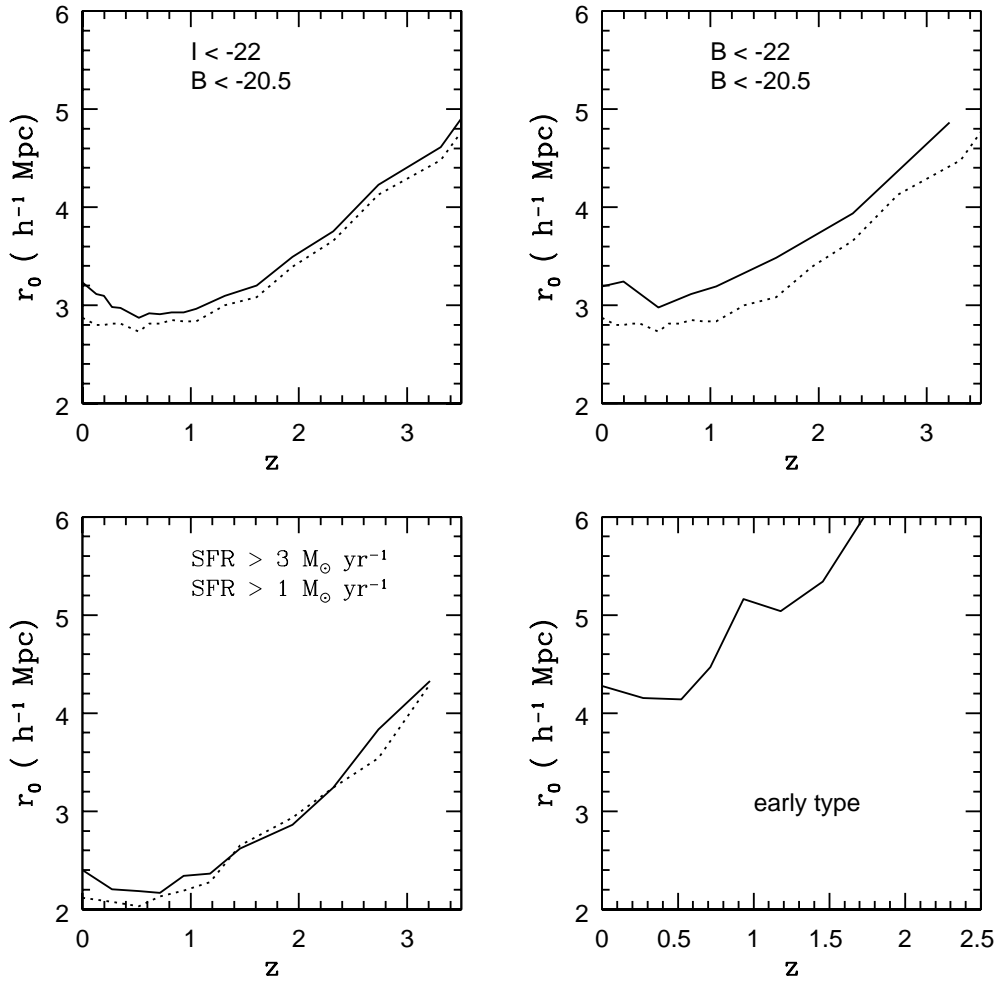


Figure 7: As in figure 6, except for the  $\tau$ CDM model.

## 4.1 What can be learned from these dependences?

We now explain *why* the evolution of clustering depends on sample selection and *what* can be learned about galaxy formation by studying the observed evolution as a function of morphological type, luminosity, colour and star formation rate.

For a given cosmology, the clustering amplitude predicted for a sample of galaxies depends on the masses of the dark matter halos they inhabit. The evolution of clustering depends on how the mass distribution of these halos changes with redshift. Additional relevant and observationally accessible information comes from the variation with redshift of the abundance of galaxies in the sample.

As an example, let us suppose that galaxies with fixed star formation rate are found in smaller halos at high redshift than at the present day. We would expect the clustering amplitude of a SFR-selected sample to show a stronger dip than a sample of galaxies that tracked halos of the same mass at all redshifts. We would also expect the abundance of galaxies in a SFR-selected sample to increase more strongly with redshift, because there are many more small halos than large ones.

As a second example, let us suppose that early type galaxies are found primarily in massive halos at all redshifts. As seen in figure 1, these galaxies should not exhibit any dip in clustering and their abundances should decrease strongly at high redshifts because massive halos are rare objects at early times.

These points are illustrated in detail in figure 8, where we plot the evolution of the median halo mass and the comoving number density of galaxies in samples selected in different ways from the  $\Lambda$ CDM simulation. The top 3 panels show results for galaxies selected according to rest-frame B-magnitude, rest-frame I-magnitude and star formation rate. At  $z = 0$ , all three galaxy samples have the same abundance and occur in halos of roughly the same mass. Galaxies selected according to star formation rate move to smaller halos at higher redshift. This effect is simply a result of the parametrization of star formation in our models. Following Kennicutt (1998), we have adopted a star formation law of the form  $\dot{M}_* = \alpha M_{cold}/t_{dyn}$ , where  $M_{cold}$  is the mass of cold gas in the galaxy and  $t_{dyn}$  is the dynamical time of the galaxy. Since  $t_{dyn}$  decreases at higher redshifts, the star formation rates are higher in halos of the same cold gas content. Galaxies selected in the B-band exhibit a weaker trend towards low-mass halos. In the case of the I-band selection, galaxies trace halos of roughly the same mass at all redshifts below 2. This is because the I-band magnitude of a galaxy is a measure of its total stellar mass, rather than its instantaneous star formation rate. We thus conclude that SFR-selected samples show the strongest dip in clustering in figure 6 because this selection procedure favours galaxies in lower mass halos at high redshift. Note that galaxies in the SFR-selected samples also exhibit the strongest increase in abundance from  $z = 0$  to  $z = 1.5$ .

The bottom two panels in figure 8 show that very bright galaxies and early-type galaxies in the simulation are found in halos with masses  $\sim 10^{13} M_\odot$ . As seen in figure 1, the clustering of these objects evolves very little from  $z = 0$  to  $z = 1$ .

In figure 9, we show the evolution of galaxy abundances and median halo masses for samples selected in the same way from the  $\tau$ CDM simulation. The results are qualitatively similar to those found for  $\Lambda$ CDM.  $L_*$  galaxies occur in halos of roughly the same masses

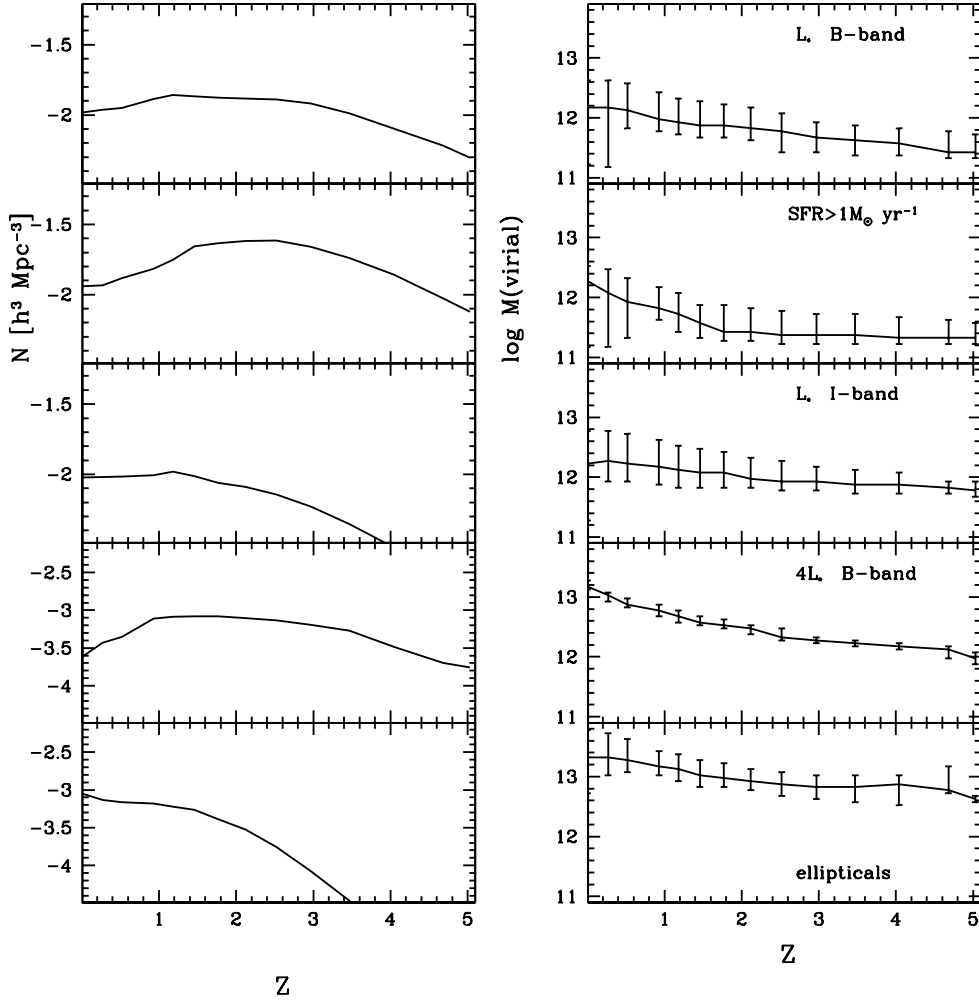


Figure 8: The evolution of the comoving number density (left column) and the median halo mass (right column) of galaxies selected from the  $\Lambda$ CDM simulation. Error bars indicate the upper and lower quartiles of the halo mass distributions. Results are shown for the selection criteria described in the caption to figure 6.

( $\sim 10^{12} M_{\odot}$ ) in both models. The reason why no dip is seen in the  $\tau$ CDM model is because halos of these masses are more strongly biased at  $z = 1$  than in the  $\Lambda$ CDM model and the decrease in halo mass with redshift for the SFR-selected sample is less pronounced. Note also that the redshift at which the abundance curves peak is higher for  $\Lambda$ CDM than for  $\tau$ CDM. In the  $\Lambda$ CDM simulation, the abundance of early-type galaxies only decreases substantially at redshifts greater than 1.5, whereas in the  $\tau$ CDM simulation, the abundance of ellipticals has already declined by a factor of 3 by  $z = 1$ .

## 5 Evolution of the slope of $\xi(r)$

Figure 10 shows the evolution of the slope  $\gamma$  of the two-point correlation function for galaxies with rest-frame B-magnitudes brighter than  $-19 + 5 \log h$  in the  $\Lambda$ CDM and  $\tau$ CDM models. We have fit a power-law to  $\xi(r)$  over three different ranges in scale:  $r = 1 - 5 \text{ h}^{-1} \text{ Mpc}$ ,  $r = 5 - 10 \text{ h}^{-1} \text{ Mpc}$  and  $r = 1 - 10 \text{ h}^{-1} \text{ Mpc}$ .

In the  $\Lambda$ CDM model, the evolution of the slope is stronger on small scales. Over the range  $1 - 5 \text{ h}^{-1} \text{ Mpc}$ ,  $\gamma$  evolves from  $-2$  at  $z = 0$  to  $-1.5$  at  $z = 1$ . On large scales,  $\gamma$  remains approximately constant. Over the range  $1 - 10 \text{ h}^{-1} \text{ Mpc}$ ,  $\gamma$  evolves from  $-1.85$  at  $z = 0$  to  $-1.6$  at  $z = 1$  and then remains constant. These results appear to be in qualitative agreement with the observations (Postman et al 1998). These authors find no dependence of  $\gamma$  on magnitude for the bright ( $I < 21$ ) galaxies in their survey. At fainter magnitudes  $\gamma$  flattens, reaching a value of  $-1.6$  at  $I=22.5$ . They also find that the flattening is stronger on smaller angular scales. Neuschaeffer & Windhorst (1995) find similar results from an independent survey carried out at a different wavelength. In the  $\tau$ CDM model, there is very little change in the slope with redshift on any scale.

## 6 Evolution of pairwise peculiar velocities

Estimates of dynamical quantities such as  $\Omega$  or cluster M/L ratios from galaxy data require knowledge not only of the spatial bias in the galaxy distribution, but also of any possible bias in the kinematics of the galaxies relative to those of the dark matter. In Paper I we explored this “velocity bias” for our  $z = 0$  models using pairwise velocity statistics, and in Paper III (Diaferio et al 1998) we will do the same using group and cluster velocity dispersions. Here we briefly explore the predicted evolution of velocity bias using pairwise statistics. The thin solid lines in figure 11 show the redshift evolution of the pairwise peculiar velocity dispersion  $\sigma_{12}$  evaluated at relative separations  $r = 0.5, 1$  and  $2 \text{ h}^{-1} \text{ Mpc}$  (co-moving units) for galaxies with rest-frame B-band magnitudes less than  $-19 + 5 \log h$  in the  $\Lambda$ CDM and  $\tau$ CDM simulations. The thick solid lines show the evolution of  $\sigma_{12}$  for the dark matter. In order to compare the *relative change* in  $\sigma_{12}$  as a function of redshift in the two models, we scale the results by dividing by the value of  $\sigma_{12}^{gal}$  at  $z=0$ . As shown in figure 13 of Paper I,  $\sigma_{12}^{gal} \simeq 800 \text{ km s}^{-1}$  ( $r = 1 \text{ h}^{-1} \text{ Mpc}$ ) in both the  $\Lambda$ CDM and  $\tau$ CDM models at the present day.

The pairwise peculiar velocities of the galaxies follow those of the dark matter quite closely in both models. The galaxy velocities are 10-40% lower than those of the dark matter at

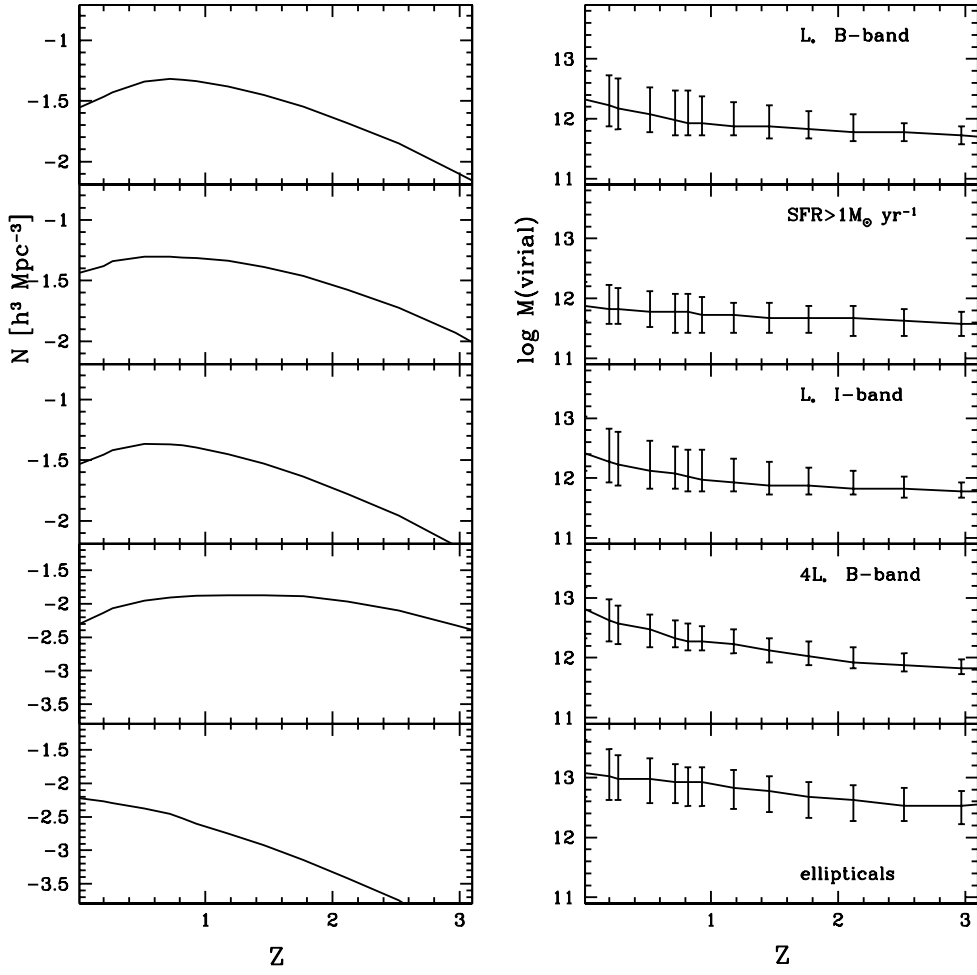


Figure 9: As in figure 8, except for the  $\tau$ CDM simulation.

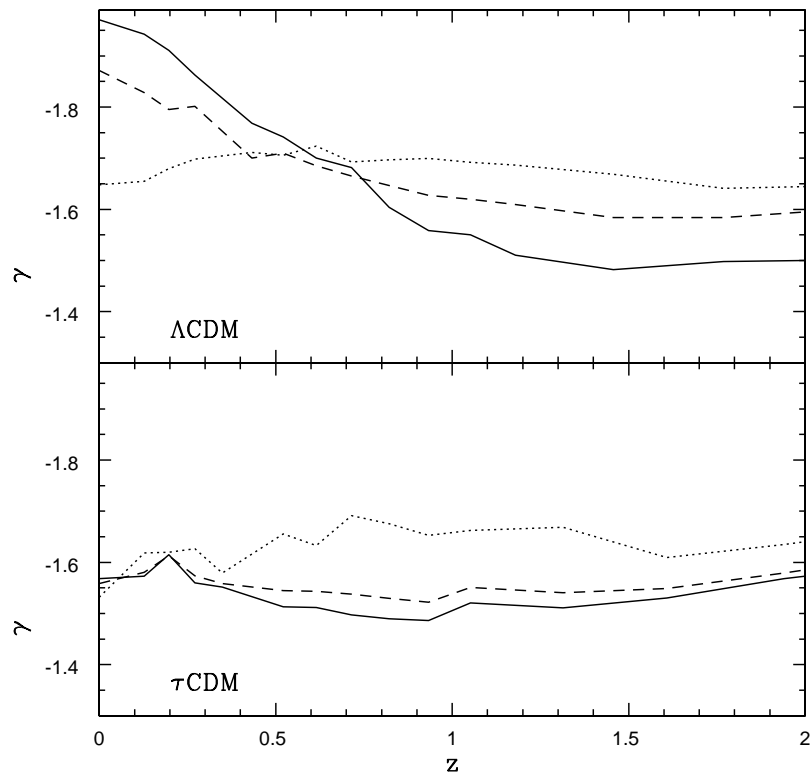


Figure 10: The evolution of the slope of the correlation function of galaxies with  $M(B) < -19 + 5 \log h$  in the  $\Lambda$ CDM and  $\tau$ CDM simulations. The solid line is the result of a fit to  $\xi(r)$  over scales between 1 and 5  $h^{-1}$  Mpc, the dotted line is for scales between 5 and 10  $h^{-1}$  Mpc and the dashed line for scales between 1 and 10  $h^{-1}$  Mpc.

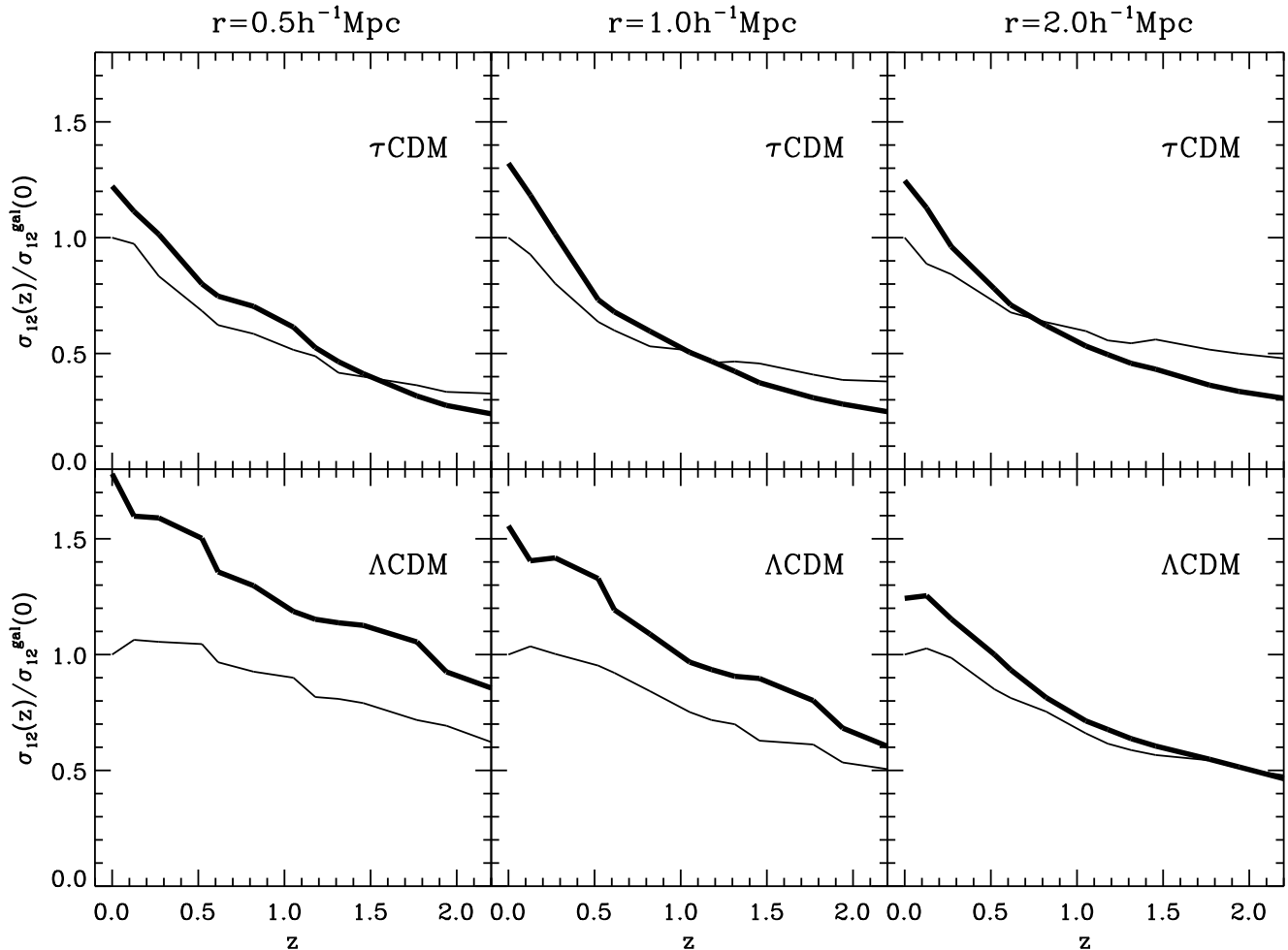


Figure 11: Redshift evolution of the pairwise velocity dispersion  $\sigma_{12}$  at relative comoving separations of 0.5, 1 and 2  $h^{-1}$  Mpc for galaxies with rest-frame B-magnitudes brighter than  $-19 + 5 \log h$  (thin lines) and for dark matter (thick lines) in the  $\Lambda$ CDM and  $\tau$ CDM simulations. The results are scaled by dividing by the value of  $\sigma_{12}^{gal}$  at  $z = 0$ .

$z = 0$ . (Note that the “antibias” in galaxy peculiar velocities at  $z = 0$  is stronger than that shown in figure 13 of Paper I, because the models presented in this paper do not include dust extinction. Dust reduces the contribution of star-forming field galaxies in a B-selected sample, but has little effect on early-type galaxies in rich groups and clusters. Models that include dust extinction thus give values of  $\sigma_{12}^{gal}$  that are 10-25 % larger ). The difference between the galaxy and dark matter peculiar velocities decreases at higher redshift. In contrast to the spatial distributions, galaxy peculiar velocities in our models are never very strongly biased. In the  $\tau$ CDM model, there is nearly a factor 2 decrease in  $\sigma_{12}^{gal}$  from  $z=0$  to  $z=0.5$ . In the  $\Lambda$ CDM models,  $\sigma_{12}^{gal}$  remains roughly constant out to  $z = 0.5$ , before decreasing at higher redshift.

## 7 Discussion and Conclusions

In a hierarchical Universe, the evolution of galaxy clustering depends on the following:

1. Cosmological parameters, such as  $\Omega$ ,  $\Lambda$  and  $\sigma_8$ , because these determine the rate at which structure grows and the epoch at which halos of given mass change from being rare objects, and thus biased tracers of the dark matter distribution, to being “typical” objects with clustering properties similar to that of the mass.
2. The relationship between the mass of a dark matter halo and the properties of the galaxies that form within it. Note that this relationship depends *only* on halo mass and is independent of the environment in which the halo finds itself (Lemson & Kauffmann 1998).
3. The evolution of the galaxy population with redshift (and hence the evolution of the relationship between galaxy properties and halo mass).

In this paper, we illustrate how differences in clustering evolution between galaxies of differing luminosity, colour, morphological type and star formation rate may help constrain galaxy formation models, and perhaps even cosmological parameters.

One interesting diagnostic that we highlight is the “dip” in correlation amplitude observed between  $z = 0$  and  $z = 1$ . We show that this dip occurs naturally in a  $\Lambda$ CDM model, where structure forms early and halos with masses in the range  $10^{11} - 10^{12} M_{\odot}$ , which contain galaxies of intermediate luminosities, are unbiased tracers of the mass over this redshift range. In the  $\tau$ CDM model, bias evolves rapidly, and the clustering amplitude of  $L_*$  galaxies remains constant from  $z = 0$  to  $z = 1$ . Although it might be possible to “force” a dip in clustering in the  $\tau$ CDM model by requiring that  $L_*$  galaxies form in less massive halos, it would be difficult to come up with a physically-motivated scheme for doing this that would not simultaneously produce too many bright galaxies.

We also show that the strength of the dip in the  $\Lambda$ CDM model is sensitive to sample selection. If galaxies are selected according to star formation rate rather than B-band luminosity, objects in low mass halos contribute more to the clustering signal at high redshifts and the dip is stronger. If galaxies are selected in the red rather than the blue, the dip is reduced. Very luminous galaxies and massive early-type galaxies exhibit no dip in clustering between  $z = 0$  and  $z = 1$  because they occur in high mass halos ( $10^{13} - 10^{14} M_{\odot}$ ) that are already biased at  $z = 0$  and become substantially more biased at high redshift.

The predictions presented in this paper should be viewed as illustrative rather than quantitative. As discussed in Paper I, the precise relation between the mass of a halo and the properties of the galaxies that form within it depends strongly on the adopted recipes for star formation and feedback; these are very uncertain. The exciting prospect is that future observations of galaxy clustering at high redshift will place strong *empirical* constraints on these processes.

## Acknowledgments

The simulations in this paper were carried out at the Computer Center of the Max-Planck Society in Garching and at the EPPC in Edinburgh. Codes were kindly made available by the Virgo Consortium. We especially thank Adrian Jenkins and Frazer Pearce for help in carrying them out. We are also grateful to John Peacock for useful discussions. A.D. is a

Marie Curie Fellow and holds grant ERBFMBICT-960695 of the Training and Mobility of Researchers program financed by the EC.

## References

- Adelberger, K.L., Steidel, C.C., Giavalisco, M., Dickinson, M., Pettini, M. & Kellogg, M., 1998, astro-ph/9804236
- Bagla, J.S., 1998a, MNRAS, 297, 251
- Bagla, J.S., 1998b, astro-ph/9711081
- Baugh, C.M., Cole, S., Frenk, C.S. & Lacey, C.G., 1998, ApJ, 498, 504
- Brainerd, T.G. & Villumsen, J.V., 1994, ApJ, 431, 477
- Carlberg, R.G., Yee, H.K.C., Morris, S.L., Lin, H., Sawicki, M., Wirth, G., Patton, D., Shepherd, C.W. et al, 1998, astro-ph/9805131
- Coles, P., Lucchin, F., Matarrese, S. & Moscardini, L., 1998, astro-ph/9803197
- Connolly, A.J., Csabai, I., Szalay, A.S., Koo, D.C., Kron, R.G. & Munn, J.A., 1995, AJ, 110, 2655
- Giavalisco, M., Steidel, C.C., Adelberger, K.L., Dickinson, M., Pettini, M. & Kellogg, M., 1998, ApJ, 503, 543
- Governato, F., Baugh, C.M., Frenk, C.S., Cole, S. & Lacey, C.G., 1998, Nature, 392, 359
- Hamilton, A.J., Kumar, P., Lu, E. & Matthews, S.A., 1991, ApJ, 374, L1
- Jain, B., Mo, H.J. & White, S.D.M., 1995, MNRAS, 276, L25
- Jenkins, A., Frenk, C.S., Pearce, F.R., Thomas, P.A., Colberg, J.M., White, S.D.M., Couchman, H.M.P., Peacock, J.A., Efstathiou, G. & Nelson, A.H., 1998, ApJ, 499, 20
- Jing, Y.P. & Suto, Y., 1998, ApJ, 494, 5
- Kauffmann, G., Colberg, J.M., Diaferio, A. & White, S.D.M., 1998, astro-ph/9805283
- Kaiser, N., 1984, ApJ, 284, 9
- Kennicutt, R.C., 1998, ApJ, 498, 541
- Le Fèvre, O., Hudon, D., Lilly, S.J., Crampton, D., Hammer, F. & Tresse, L., 1996, ApJ, 461, 534
- Lemson, G. & Kauffmann, G., 1998, astro-ph/9710125
- Ma, C.P., 1998, astro-ph/9808130
- Matarrese, S., Coles, P., Lucchin, F. & Moscardini, L., 1997, MNRAS, 286, 115
- Mo, H.J. & Fukugita, M., 1996, APJ, 467, L9

- Mo, H.J., Mao, S. & White, S.D.M., 1998, astro-ph/9807341
- Mo, H.J. & White, S.D.M., 1996, MNRAS, 282, 347
- Neuschaeffer, L.W. & Windhorst, R.A., 1995, ApJ, 439, 14
- Peacock, J.A. & Dodds, S.J., 1994, MNRAS, 267, 1020
- Postman, M., Lauer, T.R., Szapudi, I. & Oegerle, W., astro-ph/9804141
- Roukema, B.F., Peterson, B.A., Quinn, P.J. & Rocca-Volmerange, B., 1997, MNRAS, 292, 835
- Somerville, R.S., Primack, J.R. & Faber, S.M., astro-ph/9806228
- Steidel, C.C., Adelberger, K.L., Dickinson, M., Giavalisco, M., Pettini, M. & Kellogg, M., 1998a, ApJ, 492, 428
- Steidel, C.C., Adelberger, K.L., Giavalisco, M., Dickinson, M.E., Pettini, M. & Kellogg, M., 1998b, astro-ph/9805267
- Vogt, N.P., Forbes, D.A., Phillips, A.C., Gronwall, C., Faber, S.M., Illingworth, G.D. & Koo, D.C., 1996, ApJ, 465, 15
- Wechsler, R.H., Gross, M.A.K., Primack, J.R., Blumenthal, G.R. & Dekel, A., 1998, astro-ph/9712141